Rahmati, A.; Varedi-Koulaei, S. M.; Ahmadi, M. H.; Ahmadi, H.

Article

Dimensional synthesis of the Stirling engine based on optimizing the output work by evolutionary algorithms

Energy Reports

Provided in Cooperation with:
Elsevier

Suggested Citation: Rahmati, A.; Varedi-Koulaei, S. M.; Ahmadi, M. H.; Ahmadi, H. (2020) : Dimensional synthesis of the Stirling engine based on optimizing the output work by evolutionary algorithms, Energy Reports, ISSN 2352-4847, Elsevier, Amsterdam, Vol. 6, pp. 1468-1486,
https://doi.org/10.1016/j.egyr.2020.05.030

Energy Reports 6 (2020) 1468–1486

Contents lists available at ScienceDirect

Energy Reports

journal homepage: www.elsevier.com/locate/egyr

Research paper

Dimensional synthesis of the Stirling engine based on optimizing the output work by evolutionary algorithms

A. Rahmati, S.M. Varedi-Koulaei *, M.H. Ahmadi *, H. Ahmadi

Faculty of Mechanical And Mechatronics Engineering, Shahrood University of Technology, Shahrood, Iran

ARTICLE INFO

Article history:
Received 2 March 2020
Received in revised form 29 May 2020
Accepted 30 May 2020
Available online xxxx

Keywords:
Stirling engine's mechanism
Dimensional synthesis
Kinematic modeling
Output work
Schmidt theory

ABSTRACT

Nowadays, attractions are focused on Stirling engines because of their low noise, external combustion, and the possibility of employing solar energy. These engines can be designed and applied in cases of low or high-temperature differences, as needed. Evidently, the cylinder's layouts and how they are arranged and the used movement mechanism can affect the engine performance. Experts and Engineers are always looking to increase efficiency and also increase the output work of the Stirling engines. In this study, the dimensional synthesis of the kinematic chain using in the Stirling engine will be discussed. For this purpose, kinematic relationships of different layouts of Stirling are extracted, and by optimizing the mechanism based on the maximum output work, the optimal values of the geometrical parameters of the mechanism and the lengths of its links are obtained. Evolutionary optimization Algorithms, including genetic algorithm, particle swarm optimization, and imperialist competition algorithm methods are employed to optimize the problem, and their obtained results are compared. The problem is solved for four different layouts of the Stirling engine. Based on the results, the output work can be increased 9 to 14 times by varying the geometrical parameters of the Stirling engine mechanism without considering changes in thermodynamic parameters, high-temperature, and low-temperature values. Moreover, average improvement (between three optimization algorithms) for output work is about 13.05, 9.14, 10.71 and 14.36 times for α type with slider-crank, β type with slider-crank, γ type with slider-crank and α type with Ross-Yoke, respectively. Therefore, the α type Stirling engine has better advance than β and γ types, for maximizing the output work based on changing the geometrical parameters.

1. Introduction

Reduction in the amount of fossil fuels resources which is integrated with environmental pollution causing by combustion of these kinds of fuels is caused to reduce their utilization and started to replace clean and renewable fuels such as solar energy, geothermal energy, etc. as an alternative option for conventional fossil fuels (Ahmadi et al., 2019, 2018). As a result, various industries are also working to make the most of these clean, renewable, and free energy by conducting extensive research and creating the right atmosphere. Mechanical engines, such as gasoline and diesel engines, have a significant share in the use of fossil fuels due to their high usage in the modern era. Researchers are studying how to find a replacement for these engines that can provide simple utilization of renewable energy and have more scientific and economic justification. In this regard, the Stirling engine has received much attention recently (Babaelahi and Sayyaadi, 2014; Martini, 1983; Toghyani et al., 2014; Duan et al., 2014; Bayón et al., 2002; Bayon and Suarez, 2000; Boubaker et al., 2013; Motsa and Shateyi, 2012; Finkelstein, 0000; Deac, 1994; Tlili et al., 2008; Ahmadi et al., 2017; Abuelyamen et al., 2017; Almajri et al., 2017; Xiao et al., 2017a; Cheng and Yu, 2011; S et al., 2007; S. Scollo et al., 2013; Liao and Lin, 2015; Hooshang et al., 2015). Due to its structure and performance, renewable fuels, especially solar-generated fuels, can be applied in these engines (Kongtragool and Wongwises, 2003; Hachem et al., 2018).

The Stirling engine is a closed-loop external combustion engine that its operating fluid never leaves the cylinders of the engine (Ahmadi et al., 2013a,b). The external combustion feature brings about the possibility to power this engine utilizing renewable fuels (Ahmadi et al., 2013c,d). This engine can be used in cases where a low-noise engine such as submarines is needed because it generates very low volume sound density (Ahmadi et al., 2016).

The first prototype of this engine was introduced by Dr. Robert Stirling in 1816. Schmidt (Walker, 1980) introduced the first thermodynamic model to simulate the performance of a real Stirling engine, assuming that the compression and expansion processes

* Corresponding authors.
E-mail addresses: varedi@shahroodut.ac.ir (S.M. Varedi-Koulaei), mohammadhosein.ahmadi@gmail.com (M.H. Ahmadi).

https://doi.org/10.1016/j.egyr.2020.05.030

occur under isothermal conditions. Urieli and Berchowitz (1984) developed the adiabatic model of Stirling engines using numerical calculations, considering that in high-speed engines, these processes, expansion and compression, tend to be performed in adiabatic mode. Babaelahi and Sayyadi considered mechanical friction and heat loss and introduced a new numerical thermal model called Simple-II. This model, which was examined by the Lewis Research Center, was found to be more similar to the actual model (Babaelahi and Sayyaadi, 2014; Martini, 1983). Some researchers have modeled the engine with CFD models and achieved good results (Abuelyamen et al., 2017; Almajri et al., 2017; Xiao et al., 2017a). The thermodynamic analysis is not capable of investigating the transient mode of the engine. Cheng and Yu et al. As well as Scollo et al. combined the dynamic relationships of the engine with the thermodynamic equations. This combination made it possible to calculate the transient state, instantaneous mass effects of wheel flash inertia, initial rotation speed, initial load pressure, hot and cold source temperature, phase angle, and piston displacement rate (Cheng and Yu, 2011; S et al., 2007; S. Scollo et al., 2013). Bataineh has proposed a combined thermodynamic and dynamic model for the α-type Stirling engine with the Ross-Yoke mechanism (Bataineh, 2018). Moreover, He had a parametric study to investigate the effect of geometric and operation parameters on engine performance, including the effects of regenerator effectiveness, the dead volume ratio, the heat source temperature, and the swept volume ratio. Researchers need to analyze these difficult differential equations to optimize the Stirling engine. Instead of solving complex equations for the Solar Stirling engine, Liao and Lin developed a simple mathematical model using the irreversible thermodynamic method and the Lagrangian coefficient (Liao and Lin, 2015). Shendage et al. have designed and developed a β-type Stirling engine with a rhombus mechanism by considering the combined effect of the net output power and efficiency as the objective function (Shendage et al., 2017). Moreover, Altin et al. have proposed the α-type Stirling engine concept based on Scotch-Yoke linkage with parallel cylinders (Altin et al., 2018). In their research, by using a thermodynamic–dynamic simulation program, some thermodynamic and dynamic features of the engine were studied. In addition, the output power of the engine was optimized concerning the area ratio of pistons, the crank radius ratio of pistons, and the phase angle. Hooshang et al. (2015) used a multi-layer perceptron in order to calculate the maximum output work and efficiency. The authors considered the phase angle, stroke, and operating frequency of the engine as design variables.

Ding et al. have presented an advanced model based on the ideal adiabatic model in which various loss mechanisms, including the loss of heat and pressure in heat exchangers, are considered (Ding et al., 2018). They found that the relationship between thermal efficiency and volume ratio was not monotonic, and there exists a peak value. They also introduced optimal values of volume ratio according to the maximum thermal efficiency at different cooler and heater temperatures. Karabulut et al. have developed a Martini type free-piston Stirling engine concept and have conducted its performance analysis (Karabulut et al., 2019). Furthermore, they have optimized the input parameters of the analysis for 2500 rpm engine speed. Toghyani et al. carried out a multifunctional optimization with four design variables, including hot source temperature, stroke, average effective pressure, and engine frequency, to increase the efficiency and the output work and also reduce the pressure (Toghyani et al., 2014). Besides, some other researchers performed this study with other different algorithms (Duan et al., 2014; Bayón et al., 2002; Bayon and Suarez, 2000; Boubaker et al., 2013). Rao et al. have proposed an improved multi-objective Jaya optimization algorithm for a solar dish Stirling engine (Rao et al., 2019). The proposed approach uses an adaptive multi-team perturbation guiding Jaya (AMTPG Jaya) algorithm. They have examined the proposed algorithm using two multi-objective optimization case studies of a solar dish Stirling heat engine system and a multi-objective optimization case study of the Stirling heat pump and have got the superior results. In recent studies, Egas and Clucas (2018) studied several types of Stirling engine layouts. Regarding the pressure–volume (P–V) charts, the authors determined which of these configurations of the Stirling engines would work in what type of temperature difference. However, the effect of link length on the output results in not investigated yet. In addition, the effect of these lengths on the output power of the engine is another issue that is not discussed yet.

In this study, the four well-known layouts of the Stirling engine (Fig. 3) are considered, and the thermodynamic relations, Schmidt's theory, and the kinematic relations by neglecting the movement factor are also regarded. As the outputs of the current study, pressure, volume, the output work of the engine, and the effect of the link's length on the output power of the engine are also investigated. It is also worth checking that if the link lengths are changed, the classification of Jose Egas and Don M. Clucas is still acceptable (Egas and Clucas, 2018). Indeed, the engine's design and its optimization are based on the changes in the kinematics relations of the engine. Therefore, all the geometric parameters of each layout of the Stirling engine are considered as the design variables. Considering that the final purpose is to increase and maximize the output work of the engine, the heuristic optimization algorithms for each of the layouts are studied, and the optimal values for the links length are calculated.

2. Performance mechanisms of the Stirling engine

The Stirling engine can be divided into three categories depending on how the cylinders are connected, namely α, β and γ layouts (Urieli and Berchowitz, 1984; Egas and Clucas, 2018; Thombare and Verma, 2008). Moreover, each of these layouts can have different movement mechanisms, including slider-crank, Ross-Yoke, and rhombic mechanisms, the most important of which are briefly discussed in the following.

2.1. Different layouts of the Stirling engine

2.1.1. α type

The α layout of the Stirling engine (Fig. 1a) has two power pistons in two separate cylinders which a heater, a heat recovery, and a cooler are placed between the cylinders, respectively. The upper space of the hot piston is heated continuously and the upper space of the cold part is continuously cooled. In this type, pistons simultaneously carry out the task of expansion and compression of the fluid and also the task of fluid transfer between the hot and cold chambers (Bataineh, 2018; Thombare and Verma, 2008; Cheng and Yu, 2012).

2.1.2. β type

β layout of the Stirling engine (Fig. 1b) is the first type of layouts which was introduced by Dr. Stirling in 1816. This type has only one cylinder. Also, the power piston only has the task of expanding and compacting the fluid, and the transfer of fluid between the hot and cold compartments is defined to another part which is so similar to the piston and is called a displacer (Thombare and Verma, 2008; Cheng and Yu, 2012).

2.1.3. γ type

The γ layout of the Stirling engine (Fig. 1c) is in fact so similar to the β layout, except that separate cylinders are provided for the power piston and the displacement piston and the fluid flows between the two cylinders (Thombare and Verma, 2008; Cheng and Yu, 2012).

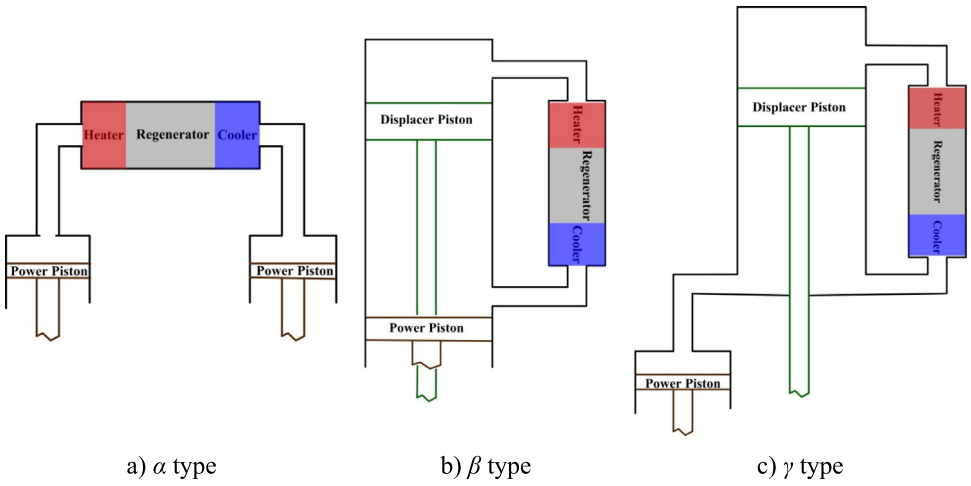

Fig. 1. Different layouts of the Stirling engine.

2.2. Stirling engine's mechanism

2.2.1. Slider-crank linkage

Slider and crank linkage (Fig. 2a) have been used in internal combustion engines for many years and it is known as a very reliable and valid mechanism. This mechanism is widely used in Stirling engines (Thombare and Verma, 2008; Cheng and Yu, 2012).

2.2.2. Ross-Yoke mechanism

The Ross-Yoke mechanism (Fig. 2b) was first introduced in 1979. Mr. Ross outlined this model to employ in an α type Stirling engine at the University of Cambridge, England. It is often used in alpha motors to reduce frictional force (Urieli and Berchowitz, 1984; Bataineh, 2018; Altin et al., 2018; Thombare and Verma, 2008; Cheng and Yu, 2012).

2.2.3. Rhombic mechanism

The Philips developed the rhombic mechanism (Fig. 2c) in 1950 for single-cylinder Stirling engines (Thombare and Verma, 2008; Cheng and Yu, 2012).

How the cylinders are connected to one another, and in particular, the mechanisms of the Stirling engine, causes the engine to operate at different temperatures. This feature is another reason for choosing a Stirling engine. Engines capable of operating at high temperatures are called the High-Temperature Difference Engine (HTD), and engines capable of operating at low temperatures are called the Low-Temperature Difference Engine (LTD) (Wang et al., 2016). In addition, these layouts will affect the output work of the engine.

Fig. 3 demonstrates the four layouts which are studied in this investigation.

3. Thermodynamic modeling

The performance cycle of the Stirling engine can be examined from two perspectives: theoretical analysis, which performs mathematical calculations on the Stirling cycle, and empirical measurements, which illustrate the actual characteristics of the cycle. The engine is designed based on the results of the mathematical and physical equations, and the obtained design is acceptable when the experimental measurements of the engine are approximately acceptable with theoretical values and meet them. The first acceptable mathematical analysis for the analysis of the Stirling cycle, fifty years after its invention, was introduced by Schmidt, known as the Schmidt theory (Urieli and Berchowitz, 1984). In this theory is assumed that the engine temperature in the hot and cold side of the engine is constant and is equal to the hot source and cold source temperature, respectively. In addition, compression and expansion processes are isothermally performed. This analysis linearizes the thermodynamic equations and makes calculations easy.

As noted in Schmidt's analysis, the key principle in this analysis is that the fluid in the expansion volume of the engine and the hot exchanger is always kept at a constant temperature equal to the temperature of the engine's hot source, and the fluid temperature in the compression volume and the cold exchanger is constant and equal to the engine's cold source. This assumption makes it possible to simplify the equations to obtain a simple relation for fluid pressure changes as a function of volume variations. The assumptions of this analysis are (Schmidt, 1871):

1. All processes are reversible.
2. The heat recovery process is ideal.
3. The working fluid follows the ideal gas state equations.
4. The fluid mass inside the system is constant and the system has no leakage.
5. Workload volumes have a sinusoidal relation with the crank angle.
6. There is no temperature change in heat exchangers.
7. The instantaneous pressure of the working fluid is the same in all engine parts.
8. The wall temperature of the cylinders and the engine piston temperature are constant.
9. The rotating parts of the engine rotate at a constant speed (the angular acceleration is zero).

If an ideal gas is used in the engine:

$$P.V = mol.R.T \tag{1}$$

where P is the absolute pressure, V denotes the volume, mol indicates the molar mass of the gas, R is the Global constant of gases, and T is the absolute temperature.

The Stirling engine is divided into 5 parts, namely Volume of compression (V_c), Cooling (k), Recovery (r), Heater (h), Volume of expansion (V_e).

Assuming the isothermally of the Schmidt theory and that there is no dead volume in any of the engine compartments including the recovery and also in the connecting tubes, the pressure can be obtained as a function of the rotation of the crank angle (β) as follows (Babaelahi and Sayyaadi, 2014):

$$P(\beta) = \frac{mol.R}{\frac{V_c(\beta)}{T_c} + \frac{Ve(\beta)}{T_e}} \tag{2}$$

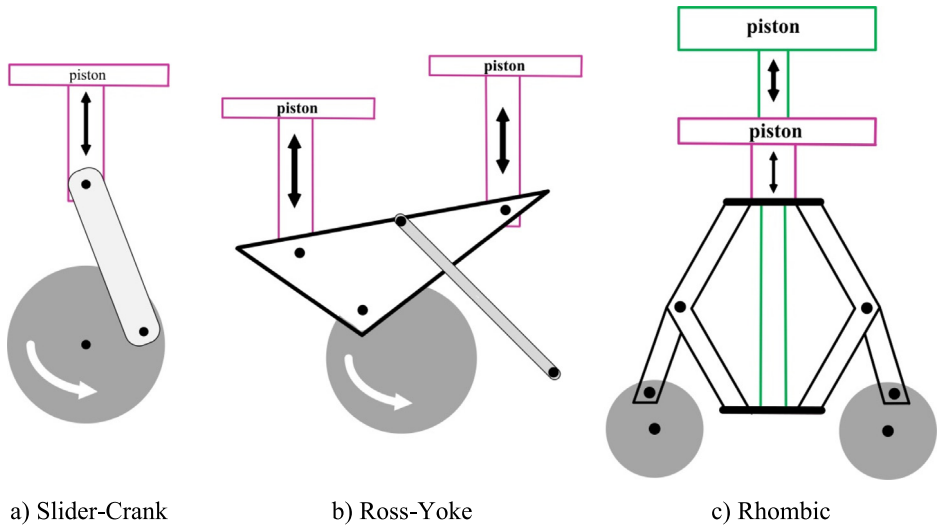

Fig. 2. The different mechanisms of the Stirling engine.

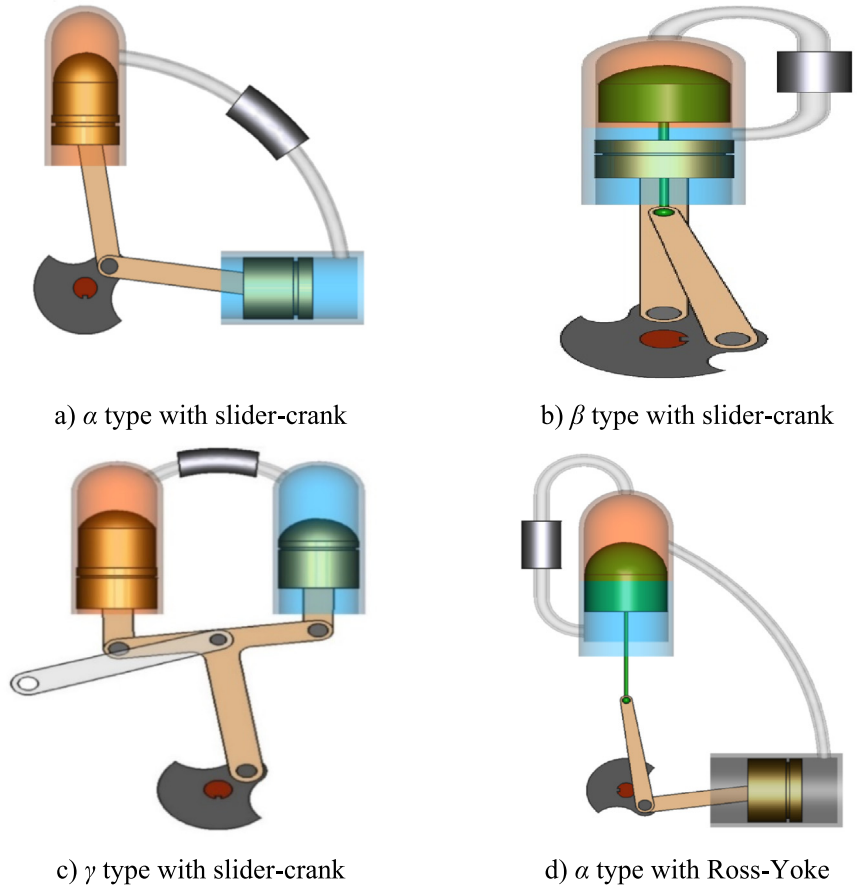

Fig. 3. Four Studied layouts of this study (Egas and Clucas, 2018).

β is the Crankshaft rotation angle, V_e and V_c are the expansion volume and compression volume in proportion to the rotation angle, and T_e and T_c denote the expansion and compression temperatures, respectively.

Using the initial conditions which are supposed to be at the standard pressure and temperature (room condition), the molar mass can be calculated from the state relation as follows:

$$mol = \frac{P_{\text{mean}}.V_{\max}}{R.T_{room}} \tag{3}$$

P_{mean} is the engine's absolute pressure in static conditions, V_{max} is the maximum engine volume, and T_{room} is the room temperature.

Each of the above volumes can be calculated for each of the layouts by using kinematic equations.

4. Kinematic modeling

Using the governing kinematic relationships of each layout, regardless of the moving factor, the compression volume (V_c)

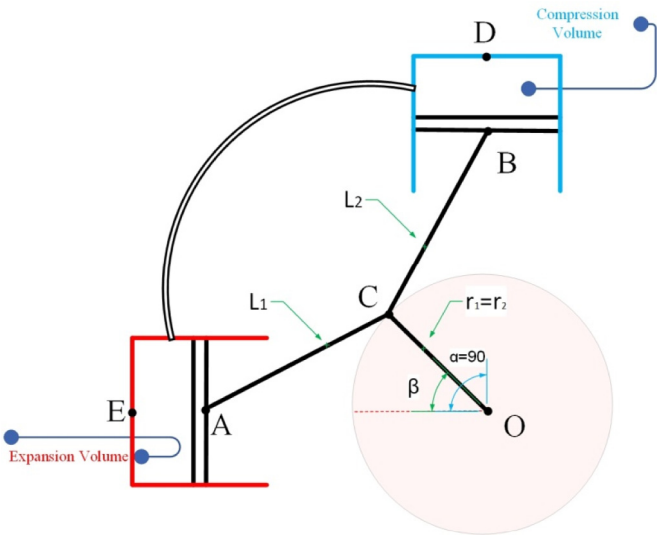

Fig. 4. α type with slider-crank linkage.

and the expansion volume (V_e) can be calculated. If the values of pressure and volume relative to the rotation angle are known, the equation of fluid pressure variations as a function of volume changes would be yielded. Given this relation, the pressure diagram in terms of the volume of the engine and the output of the engine, which is actually the area of the enclosure, can be calculated.

4.1. α type with slider-crank linkage

Regarding the geometry of the mechanism in α type Stirling engine with slider-crank linkage that is shown in Fig. 4, one can find the displacement of the pistons with β as follows:

$$AE(\beta) = OE - OA = (r_1 + l_1) - \left(r_1.\cos(\beta) + \sqrt{l_1^2 - r_1^2.\sin(\beta)^2}\right) \tag{4}$$

$$BD(\beta) = OD - OB = (r_2 + l_2) - \left(r_2.\cos(\alpha - \beta) + \sqrt{l_2^2 - r_2^2.\sin(\alpha - \beta)^2}\right) \tag{5}$$

where r_1 is the crank radius ($r_1 = r_2$), l_1 and l_2 are the lengths of the connecting rods, α indicates the phase angle, and β denotes the rotation angle of the crank relative to the horizontal surface.

Given the radius of compression (C_r) and expansion pistons (E_r), respectively:

$$V_e(\beta) = \pi.E_r^2.AE(\beta) \tag{6}$$

$$V_c(\beta) = \pi.C_r^2.BD(\beta) \tag{7}$$

Then the total volume is obtained from the expansion volume and the compression volume in the following equation:

$$V_t(\beta) = V_e(\beta) + V_c(\beta) \tag{8}$$

The minimum and maximum volumes of the engine can be obtained using derivative of the V_t relative to β by calculating the roots of the following equation:

$$\frac{d(V_t(\beta))}{d\beta} = 0 \tag{9}$$

Eq. (9) has two roots of $\beta = 45^o$, and $\beta = 225^o$. Therefore, the minimum and maximum volume equations can be calculated as follows:

$$V_{min} = V_t(\beta = 45^\circ) \tag{10}$$

$$V_{max} = V_t(\beta = 225^\circ) \tag{11}$$

Now by employing the equations of pressure and volume, the output work equation of the engine can be obtained as follows:

$$W_{(\alpha\_sc)} = \int_{\beta=45^\circ}^{\beta=225^\circ} P(\beta).\left(\frac{dV_t(\beta)}{d\beta}\right) - \int_{\beta=225^\circ}^{\beta=405^\circ} P(\beta).\left(\frac{dV_t(\beta)}{d\beta}\right) \tag{12}$$

4.2. β type with slider-crank linkage

Regarding the geometry of the mechanism in β type Stirling engine with slider-crank linkage that is shown in Fig. 5, the displacement of the pistons can be extracted as follows:

$$EG(\beta) = OG - OE = (r_2 + l_2 + C_2) - \left(C_1 + r_1.\cos(\beta) + \sqrt{(l_1^2 - r_1^2.\sin(\beta)^2)}\right) \tag{13}$$

$$FG(\beta) = OG - OF = (r_2 + l_2 + C_2) - \left(C_2 + r_2.\cos(\beta + \alpha) + \sqrt{l_2^2 - r_2^2.\sin(\beta + \alpha)^2}\right) \tag{14}$$

where r_1 is the radius of the crank ($r_1 = r_2$), l_1 and l_2 are the lengths of the connecting rods, C_1 and C_2 indicate the pistons lengths, α is the phase angle, and β denotes the rotation angle of the crank relative to the horizon.

In this case, the expansion volume and the total volume are obtained using the expansion piston radius (E_r):

$$V_e(\beta) = \pi.E_r^2.FG(\beta) \tag{15}$$

$$V_t(\beta) = \pi.E_r^2.EG(\beta) \tag{16}$$

Then the compression volume is obtained from the following relation:

$$V_c(\beta) = V_t(\beta) - V_e(\beta) \tag{17}$$

Therefore, The minimum and maximum volumes are the roots of the derivative of Eq. (17):

$$\frac{d(V_t(\beta))}{d\beta} = 0 \tag{18}$$

Eq. (18) has two roots of $\beta = 0^o$ and $\beta = 180^o$, which are used for extreme values of the engine volume. Then, the minimum and maximum volume equations can be calculated as follows:

$$V_{min} = V_t(\beta = 0^\circ) \tag{19}$$

$$V_{max} = V_t(\beta = 180^\circ) \tag{20}$$

With the pressure and volume equations, the output work of the engine can be simply calculated as follows:

$$W_{(\beta\_sc)} = \int_{\beta=0^\circ}^{\beta=180^\circ} P(\beta).\left(\frac{dV_t(\beta)}{d\beta}\right) - \int_{\beta=180^\circ}^{\beta=360^\circ} P(\beta).\left(\frac{dV_t(\beta)}{d\beta}\right) \tag{21}$$

4.3. γ type with slider-crank linkage

Due to the geometry of the mechanism in Fig. 6 that are based on the γ type Stirling engine with slider-crank linkage, the

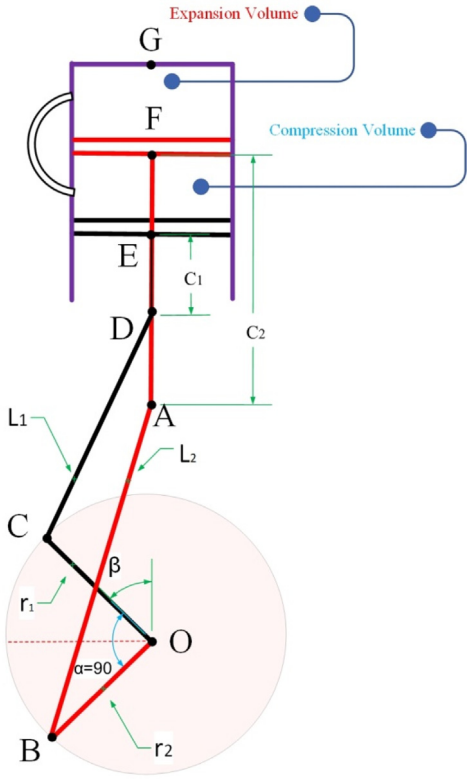

Fig. 5. β type with slider-crank linkage.

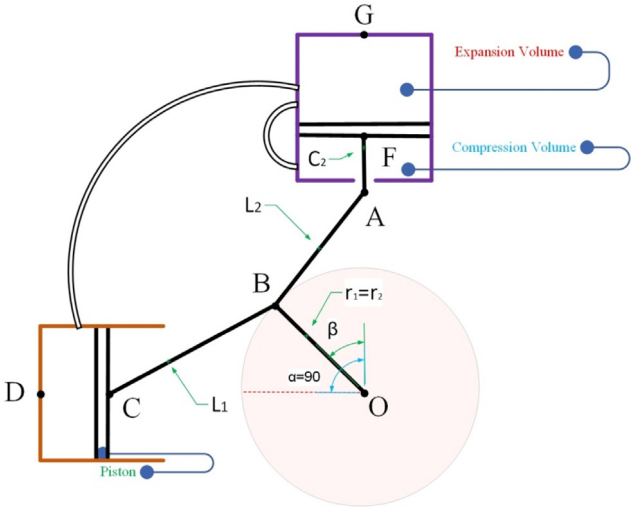

Fig. 6. γ type with slider-crank linkage.

position of the pistons can be extracted as follows:

$$FG(\beta) = OG - OF = (r_2 + l_2 + C_2) - \left(C_2 + r_2.\cos(\beta) + \sqrt{l_2^2 - r_2^2.\sin(\beta)}\right) \quad (22)$$

$$CD(\beta) = OD - OC = (r_1 + l_1) - \left(r_1.\cos(\beta - \alpha) + \sqrt{l_1^2 - r_1^2.\sin(\beta - \alpha)^2}\right) \quad (23)$$

where r_1 is the crank radius ($r_1 = r_2$), l_1 and l_2 indicate the lengths of the connecting rods, C_2 is the slider length, α denotes the phase angle, and β is the rotation angle of the crank. Given the radius of the expansion piston (E_r) and displacement piston (D_r), one can find the volumes as follows:

$$V_e(\beta) = \pi.D_r^2.FG(\beta) \quad (24)$$

$$V_c(\beta) = V_e(\beta = 180^\circ) - V_e(\beta) \quad (25)$$

Then, the total volume is obtained as follows:

$$V_t(\beta) = V_e(\beta = 180^\circ) + \pi.E_r^2.CD\,(\beta) \quad (26)$$

Similar to other cases, the minimum and maximum volumes are obtained using the derivative of Eq. (26):

$$\frac{\mathrm{d}\,(V_t\,(\beta))}{\mathrm{d}\beta} = 0 \quad (27)$$

The two roots of Eq. (27), which are $\beta = 90^o$ and $\beta = 270^o$, are used for obtaining the minimum and the maximum volume equations as follows:

$$V_{\min} = V_t\,(\beta = 90^\circ) \quad (28)$$

$$V_{\max} = V_t\,(\beta = 270^\circ) \quad (29)$$

Using the equations of pressure and volume, the output work of the engine is obtained as follows:

$$W_{(\gamma\_sc)} = \int_{\beta=90^\circ}^{\beta=270^\circ} P(\beta).\left(\frac{\mathrm{d}V_t(\beta)}{\mathrm{d}\beta}\right) - \int_{\beta=270^\circ}^{\beta=450^\circ} P(\beta).\left(\frac{\mathrm{d}V_t(\beta)}{\mathrm{d}\beta}\right) \quad (30)$$

4.4. α type with Ross-Yoke mechanism

Considering the geometry of the α type Ross-Yoke mechanism represented in Fig. 7:

$$OA(\beta) = OD - \left(-r_1.\sin(\beta) - \frac{r_1.l_2.\cos(\beta)}{2.l_1} + \sqrt{l_1^2 - r_1^2.\cos(\beta)^2}\right) \quad (31)$$

$$OB(\beta) = OD - \left(-r_1.\sin(\beta) + \frac{r_1.l_2.\cos(\beta)}{2.l_1} + \sqrt{l_1^2 - r_1^2.\cos(\beta)^2}\right) \quad (32)$$

where r_1 is the crank radius, l_1 and l_2 are the links lengths, and β is the rotation angle of the crank relative to the horizontal surface. Furthermore, OD can be calculated as follows:

$$OD = \sqrt{((l_1 + l_2)^2 + r_1)^2 - l_2^2} \quad (33)$$

The cylinders volumes are obtained using the radius of the expansion piston (E_r) and the radius of the compression piston (C_r) as follows:

$$V_e(\beta) = \pi.E_r^2.OA(\beta) \quad (34)$$

$$V_c(\beta) = \pi.C_r^2.OB(\beta) \quad (35)$$

Then, the total volume is obtained from the following equation:

$$V_t(\beta) = V_c(\beta) + V_e(\beta) \quad (36)$$

According to the previous cases, the derivative of V_t result in the minimum and maximum volumes of the engine:

$$\frac{\mathrm{d}\,(V_t\,(\beta))}{\mathrm{d}\beta} = 0 \quad (37)$$

The preceding equation, Eq. (37), has two roots of $\beta = 90^o$ and $\beta = 270^o$, which are used for extracting the minimum and

maximum volume equations as follows:

$$V_{\min} = V_t\ (\beta = 90^\circ) \tag{38}$$

$$V_{\max} = V_t\ (\beta = 270^\circ) \tag{39}$$

Then, by applying the pressure and volume equations, the output work of the engine is obtained as follows:

$$W_{(\alpha\_RY)} = \int_{\beta=90^\circ}^{\beta=270^\circ} P(\beta).\left(\frac{dV_t(\beta)}{d\beta}\right) - \int_{\beta=270^\circ}^{\beta=450^\circ} P(\beta).\left(\frac{dV_t(\beta)}{d\beta}\right) \tag{40}$$

The output work of the Stirling engine (W) for each layout is obtained from the pressure integration of the volume variations, which is equivalent to the surface enclosed in the pressure–volume (P–V) graph.

5. Optimization

The output work for each of the layouts, Eqs. (12), (21), (30), and (40), depends on the pressure and volume. Indeed, the pressure and volume equations depend on the length of the links and the radius of the cylinders. Therefore, the variation in the output work is the function of the links length and the radius of the cylinders. The output can be maximized by considering the length of the links as well as the radius of each cylinder as design parameters and by performing optimization algorithms. In other words, the geometrical parameters of the engine are selected for kinematic optimization of the engine, and the other thermodynamic parameters are considered to be fixed. Then the maximum output work can be simply achieved by using evolutionary algorithms that are used in many practical engineering problems.

In this study, the output work of the Stirling engine optimized by using the Genetic Algorithm (GA), Partial Swarm Optimization (PSO), and Imperialist Competition Algorithm (ICA), and reaches to its maximum by considering the design constraints such as maximum pressure.

5.1. GA

Among various evolutionary approaches used in the optimization of energy systems, GA is very attractive and famous (Xiao et al., 2017b; Kraitong and Mahkamov, 2011; Woon et al., 2005). Genetic Algorithm (GA) has represented by Holland and his student DeJong in 1975 (Holl, 1975), which is an applicable and global search method based on the concepts of genetics, natural selection, and evolution law of Darwin's theory, the survival of the fittest (Rao, 2019). Design variables of the problems are encoded to chromosomes, and then a random initial population is generated by the chromosomes. By the estimation of competency of the chromosomes in fitness function (objective function), offsprings are generated using three operators, namely Reproduction, Crossover, and Mutation. The fundamental operators of this approach which are based on natural genetics are as:

- Reproduction: This operator is also called the selection operator because it is used for selecting the favorable individual of the considered population. Indeed, the reproduction operator is applied to separate good individuals from the population and insert their multiple copies in the next step based on a random scheme, for instance, Roulette-wheel (Rao, 2019).
- Crossover: This operator that is the main one, is applied for new individual creation by transferring data among the mating pool individuals. In the current step, usually, two random individuals are separated from the mating pool generated by the reproduction operator, and some sections of the individuals are interchanged (Rao, 2019). This operator can be applied in the single-point or several-points crossover, based on the cutting positions.
- Mutation: This operator that has modeled the natural genetic mutation, is used for random changing some of the individuals' specifics with a small mutation probability, p_m This step of GA can be implemented in different ways, including single-point mutation, bit-wise mutation, etc. (Rao, 2019).

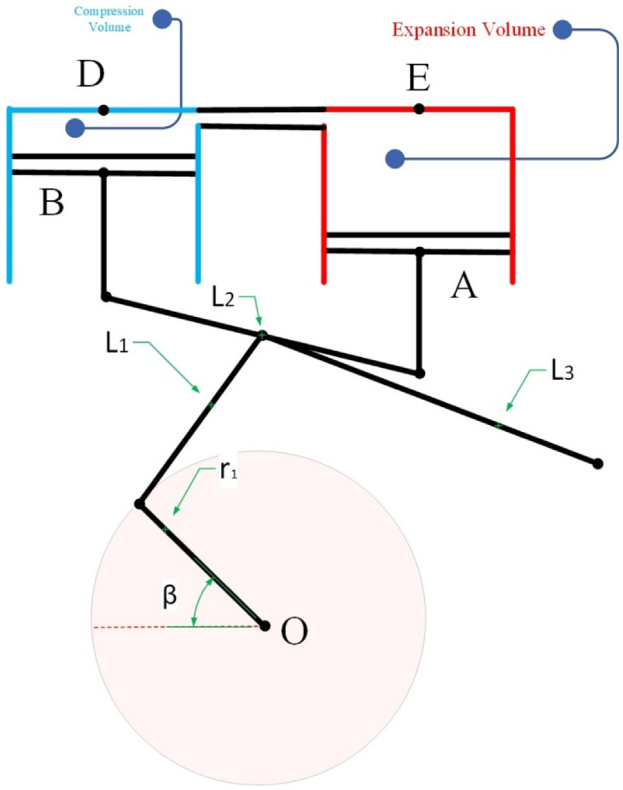

Fig. 7. α type with Ross-Yoke mechanism.

In the optimization procedure in GA is initiated based on a random population. Afterward, the mentioned operators are applied to operate the selected population in the last step in order to generate a new set of points (designs). Subsequently, the produced points or population are re-evaluated to obtain the fitness values and checked to assess convergence. In the GA method, each cycle, which consists of the mentioned three operators in addition to the assessment of fitness values, is known as a generation. Therefore, the information of the population transmits from generation to generation, and finally, the best value of the objective function is obtained as an optimized design.

5.2. PSO

PSO optimization approach, defined by Kennedy and Eberhart in 1995 (Kennedy and R., 1995), is based on bees, birds, and fish social behavior and their dynamic movement (Rao, 2019). The particle path in the swarm is dependent on their own information and knowledge in addition to swarm's knowledge and information that might be adopted during the iterations. Indeed, if a particle detects a suitable direction to food, or find a path to the maximum point in the optimization problem, the other particles of the swarm will also be able to follow this path, even

if their position is not close to the optimum point. The most appropriate location of the jth particle is named "$P_{best,j}$" while the corresponded location for the swarm is noted by "G_{best}" in all iterations. The following equations are employed for the determination of jth particle position and velocity (Sardashti et al., 2013; Praveen and Duvigneau, 2009).

$$X_j(i) = X_j(i-1) + V_j(i), j = 1, 2, \ldots, N. \quad (41)$$

$$V_j(i) = \gamma(i) V_j(i-1) + c_1 u_1 \left[P_{best,j} - X_j(i-1)\right] + c_2 u_2 \left[G_{best} - X_j(i-1)\right], j = 1, 2, \ldots, N. \quad (42)$$

c_1 and c_2 are the constants, which are known as learning coefficients of Cognitive (individual) and Social (group), respectively. The corresponded values of these constants are generally 2. Two random numbers, denoted by u_1 and u_2, which are in the range of 0 and 1, are used in the equation mentioned above. Finally, a weighting factor, which is shown by γ(i), is utilized in this approach, which can be kept constant or changes (between 0 and 1). This factor, usually, is reduced linearly by increasing the number of iterations as follows:

$$\gamma(i) = \gamma_{max} - \left(\frac{\gamma_{\max} - \gamma_{min}}{i_{\max}}\right) i \quad (43)$$

where γ_{max} and γ_{min} are the initial and final values of the weighting factor, respectively, where usually are considered as $\gamma_{max} = 0.9$ and $\gamma_{max} = 0.4$. Moreover, i_{max} is the maximum number of iterations used in the optimization process.

5.3. ICA

One of the recently-developed metaheuristic algorithms applicable to the optimization problems is called ICA. This algorithm was proposed by Atashpaz-Gargari and Lucas (2007) on the basis of imperialistic competition. In the ICA algorithm, the optimization process starts with an initial population whose individuals are based on the country type. The countries of the individuals are classified into the imperialist group and colony. These groups are originated from empires. ICA operated on the basis of imperialistic competition of the empires, which means power increment empires with more capability and reduction in the power of empires with weaker capabilities. The convergence criterion of this algorithm is remaining just one empire, which is the optimal solution; in this case, the rest countries are called the empire's colonies.

The steps of this evolutionary algorithm, which is based on the process of human social and political evolution in the imperialistic competition, can be written as follows:

— *Creation of Initial Empires*

The initial countries are produced by the size of $N_{country}$ to start the optimization algorithm. The most powerful countries are separated as the imperialists of size $N_{imp,}$ and the other countries are assumed the colonies of size N_{col}. The power of each country is related to its fitness, and each colony is assigned to imperialist countries based on its power. Indeed, an imperialist and its colonies create an empire (Atashpaz-Gargari and Lucas, 2007).

— *Assimilation*

After creating initial empires, the assimilation process begins, where the imperialist country attracts its colonies in each empire based on the language and culture. This absorption is modeled by the movement of the colonies towards imperialist (Atashpaz-Gargari and Lucas, 2007).

— *Revolution*

In the process of assimilating an empire, when a colony moves to the empire, a colony may reach a better position at a lower cost than the imperialist. Therefore, in such cases, the position of the colony and the imperialist will exchange, and therefore, the algorithm will continue with the new imperialist (Atashpaz-Gargari and Lucas, 2007).

— *Total power of an empire*

The power of an empire directly depends on the power of the imperialist and the colonies, where imperialist power is more important. Therefore, the total power of an empire can be obtained as follows (Atashpaz-Gargari and Lucas, 2007).

$$F_{(tot,n)} = Fitness(X_{imperialist_n}) + \zeta\, mean\{Fitness(X_{coloniesofempire_n})\} \quad (44)$$

where $F_{tot,n}$ is the total fitness of the nth empire, and ζ is a positive number, which is considered to be less than 1.

— *Imperialistic competition*

In the following step, all empires tend to own and control the colonies of other empires. Therefore, the competition will begin for possession of the weakest colony (or colonies) of the weakest empire by other empires. The weakest colony of the weakest empire is more likely to be possessed by the most powerful empire; in other words, this colony does not necessarily possess the most powerful empire (Atashpaz-Gargari and Lucas, 2007).

— *Elimination of the weakness Empires*

As mentioned in the previous section, the weakest colonies of the weakest imperialists are divided between the other empires. In other words, the weakest empire will lose its weakest colonies in iterations of the optimization algorithm. During the process of losing the Empire's colonies, the empire collapses and eliminates, if it loses all its colonies (Atashpaz-Gargari and Lucas, 2007).

— *Convergence of ICA*

At the end of the imperialist competition, all empires are eliminated, and only the most powerful (one) empire remains. In other words, all colonies are under the control of the most powerful empire (Atashpaz-Gargari and Lucas, 2007).

5.4. Optimization algorithms' parameters

During introducing the optimization algorithms, one can find that each algorithm has some selected parameters. The different optimization algorithms parameters used in this work are presented in Table 1. For a better comparison between optimization algorithms, the population size and the maximum number of iterations are considered the same for all algorithms.

Table 1
The used optimization algorithms' parameters.

Parameter	Method (s)	Value
Maximum number of iterations	GA PSO ICA	100
Population size	GA PSO ICA	30
Crossover coefficient	GA	0.7
Mutation coefficient	GA	0.4
Inertia weight (velocity)	PSO	0.5
Reduction factor of inertia weight	PSO	0.9
Cognitive (individual) learning coefficient	PSO	2
Social (group) learning coefficient	PSO	2
Number of imperialists	ICA	10
Assimilation coefficient	ICA	2
Revolution coefficient	ICA	0.1
Colonies mean cost coefficient	ICA	0.1

Table 2
Thermodynamic parameters values.

Parameter	Value
R	$8.314^{*}10^{3}$ cm^3 kPa/K mol
P_{mean}	101.325 kPa
T_{room}	298 K
T_c	398 K
T_e	850 K

Table 3
The permissible range of engine pressure's variations.

Variables		α type slider-crank	β type slider-crank	γ type slider-crank	α type Ross-Yoke
P (kPa)	Min	180	150	250	150
	Max	1200	700	600	3000

6. Results

In order to present and evaluate the obtained results, first, the constant values and then the constraints of each layout are specified, and then the outcomes are presented and examined.

In order to compare the layouts, the expansion and compression temperatures are assumed to be constant, the crank radiuses r_1 and r_2 are assumed to be equal, and the phase angle between the two pistons (α) is assumed to be equal to 90°. The thermodynamic parameters' values are shown in Table 2. The most important constraint for our optimization problem is the permissible range of engine pressure variations. Engine working pressure is always one of the parameters that designers must be considered in their engine design. High pressures can lead to high dynamic forces, difficulty in sealing, and less working life of engine parts. Therefore, the maximum and minimum values of engine pressure for different layouts are considered as the design constraints where are shown in Table 3. Moreover, Table 4 shows the search intervals of the design variables for different layouts. These constraints result in a suitable and practical design for the Stirling engine.

6.1. α layout with slider-crank linkage

The optimization results of this layout are demonstrated in Table 5. Furthermore, the P–V diagram for the original and optimal engines, comparison between them, and the changes in the objective function values for different iterations, using GA, PSO, and ICA algorithms, are shown in Figs. 8–10, respectively.

The important points of the optimized designs using three optimization methods are as follows:

- Crank length ($r_1 = r_2$) and expansion piston radius E_r reach the highest value.
- It can be found that regardless of other parameters, increasing the value of $r_1 = r_2$ can be lead the higher output work.
- Our several tests about pistons radiuses show that if either E_r or C_r has increased, it can result in higher output work.
- A comparison of the results of three optimization algorithms shows that the PSO result has the lowest value for l_1 and l_2 and the highest value for output work. It makes it clear that the higher value for the lengths of the links not necessarily leads to higher output work.
- The output works of the optimized mechanisms extracted using three optimization techniques are approximately 13 times greater than the original mechanism.
- PSO has the best result between three optimization techniques for this layout of the Stirling engine.

6.2. β type with slider-crank linkage

The numerical results of the optimum designs using different optimization techniques for this layout are represented in Table 6. Moreover, the P–V diagram for the original and optimal engines, comparison between them, and the changes in the objective function values for different iterations, using GA, PSO, and ICA algorithms, are shown in Figs. 11–13, respectively.

For this case of optimization, numerical results of Table 6 show that:

- Crank length ($r_1 = r_2$) and expansion piston radius E_r reach the highest value.
- It can be found that regardless of other parameters, increasing the value of $r_1 = r_2$ or E_r can be lead the higher output work.
- A comparison of the results of three optimization algorithms shows that the ICA has the highest value for output work and the lowest mean values for link's lengths. It makes it clear that the higher value for the lengths of the links not necessarily leads to higher output work.
- The output works of the optimized mechanisms extracted using three optimization techniques are approximately nine times greater than the original mechanism.
- ICA has the best result between three optimization techniques for this layout of the Stirling engine.

6.3. γ type with slider-crank linkage

The optimal values of the design variables for this layout using different optimization techniques are represented in Table 7. Furthermore, the P–V diagram for the original and optimal engines, comparison between them, and the changes in the objective function values for different iterations, using GA, PSO, and ICA algorithms, are shown in Figs. 14–16, respectively.

The values optimum data in Table 7 for the γ layout with the slider-crank linkage of the Stirling engine indicate that:

- Crank length ($r_1 = r_2$) and expansion piston radius E_r reach the highest value.
- It can be found that regardless of other parameters, increasing the value of $r_1 = r_2$ can be lead the higher output work.
- Our several tests about pistons radiuses show that if E_r has increased, it can result in higher output work, but increasing in D_r has decreased the output work.
- c_2 has not any effect on the maximization of the output work.
- A comparison of the results of three optimization algorithms shows that the ICA result has the lowest value for l_1, and C_2 and the highest value for output work. It makes it clear that the higher value for the lengths of the links not necessarily leads to higher output work.
- The output works of the optimized mechanisms extracted using three optimization techniques are approximately 10 to 11 times greater than the original mechanism.
- ICA has the best result between three optimization techniques for this layout of the Stirling engine.

6.4. α type with Ross-Yoke mechanism

Table 8 shows the optimization results of this layout. Moreover, the P–V diagram for the original and optimal engines, comparison between them, and the changes in the objective function values for different iterations, using GA, PSO, and ICA algorithms, are shown in Figs. 17–19, respectively.

Table 4
Interval search for the design variables parameters.

Variables		α type slider-crank	β type slider-crank	γ type slider-crank	α type Ross-Yoke
l_1 (cm)	Min	5	5	3	5
	Max	70	30	20	20
l_2 (cm)	Min	5	5	3	5
	Max	70	30	20	20
c_1 (cm)	Min	–	1	–	–
	Max	–	8	–	–
c_2 (cm)	Min	–	4	3	–
	Max	–	16	12	–
$r_1 = r_2$ (cm)	Min	1	1	1	1
	Max	4	4	5	4
E_r (cm)	Min	1	1	1	1
	Max	5	4	4	4
C_r (cm)	Min	1	–	–	1
	Max	8	–	–	7
D_r (cm)	Min	–	–	1	–
	Max	–	–	7	–

Table 5
Optimal values for the variables of α type with slider-crank.

	Original values Egas and Clucas (2018)	Optimal values using GA	Optimal values using PSO	Optimal values using ICA
l_1 (cm)	10	48.7836	37.7336	38.382
l_2 (cm)	10	60.3607	37.7336	62.3191
$r_1 = r_2$ (cm)	2	3.99999	4	4
E_r (cm)	2	4.99997	5	5
C_r (cm)	2	4.90692	4.99908	5.00149
W (kg(cm/s)^2)	$W_0 = 15179.4865$	196619.0045	198899.8143	198763.7692
W/W_0	1	12.9529	13.1032	13.0942

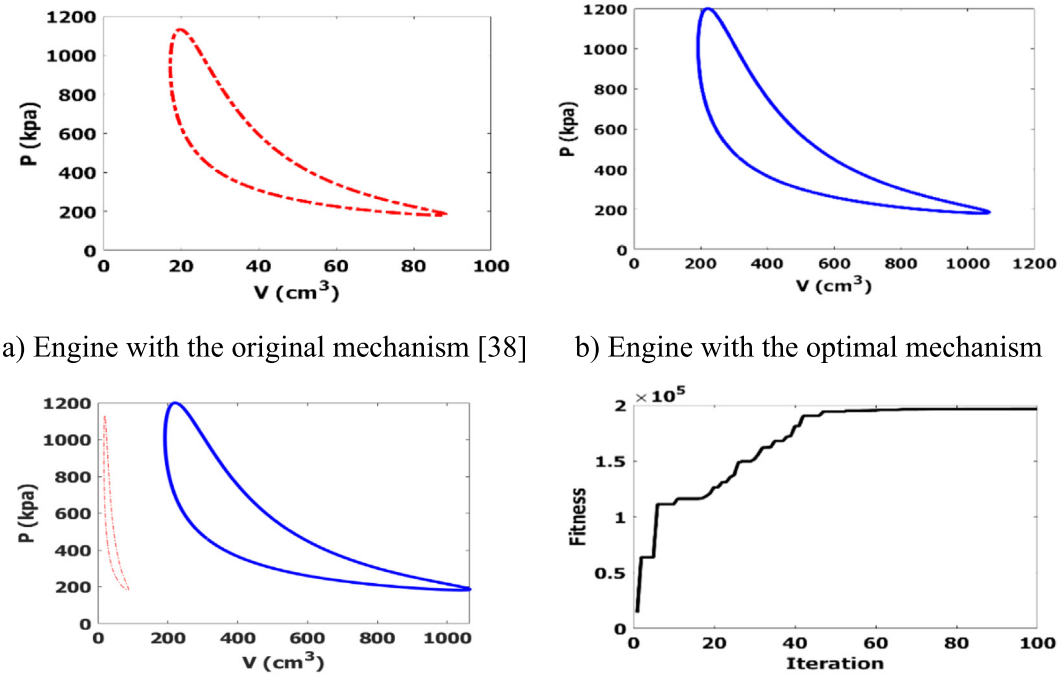

a) Engine with the original mechanism [38]

b) Engine with the optimal mechanism

c) Comparison between the original and optimal engines

d) Variations of the fitness function's values

Fig. 8. Optimization results of the α layout with slider-crank linkage using GA.

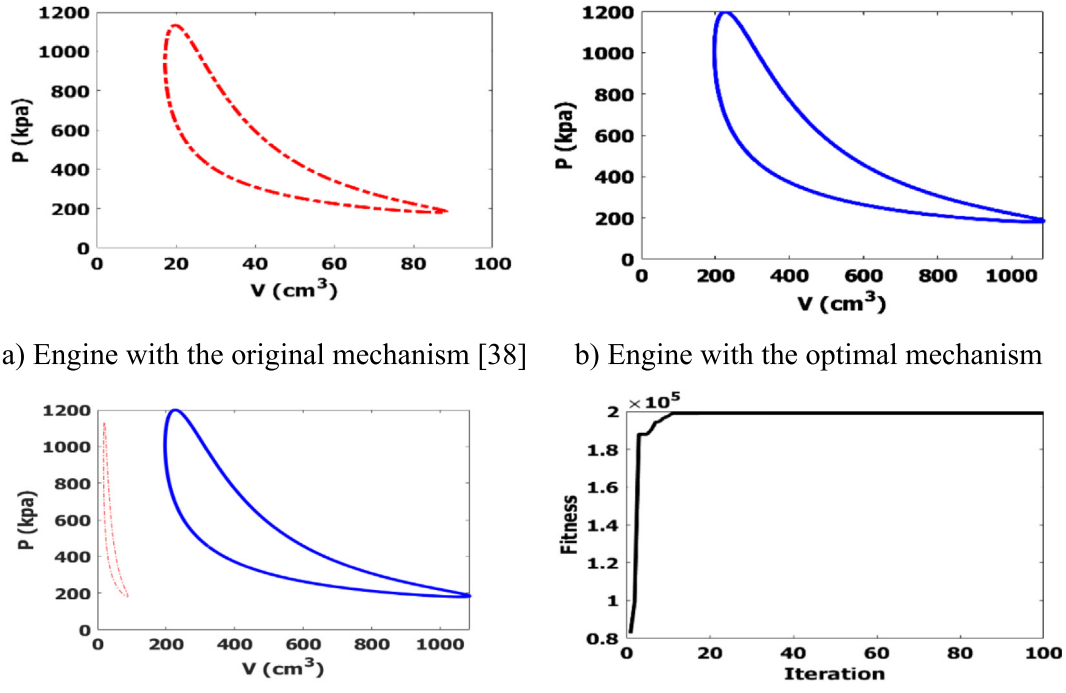

a) Engine with the original mechanism [38] b) Engine with the optimal mechanism

c) Comparison between the original and optimal engines d) Variations of the fitness function's values

Fig. 9. Optimization results of the α layout with slider-crank linkage using PSO.

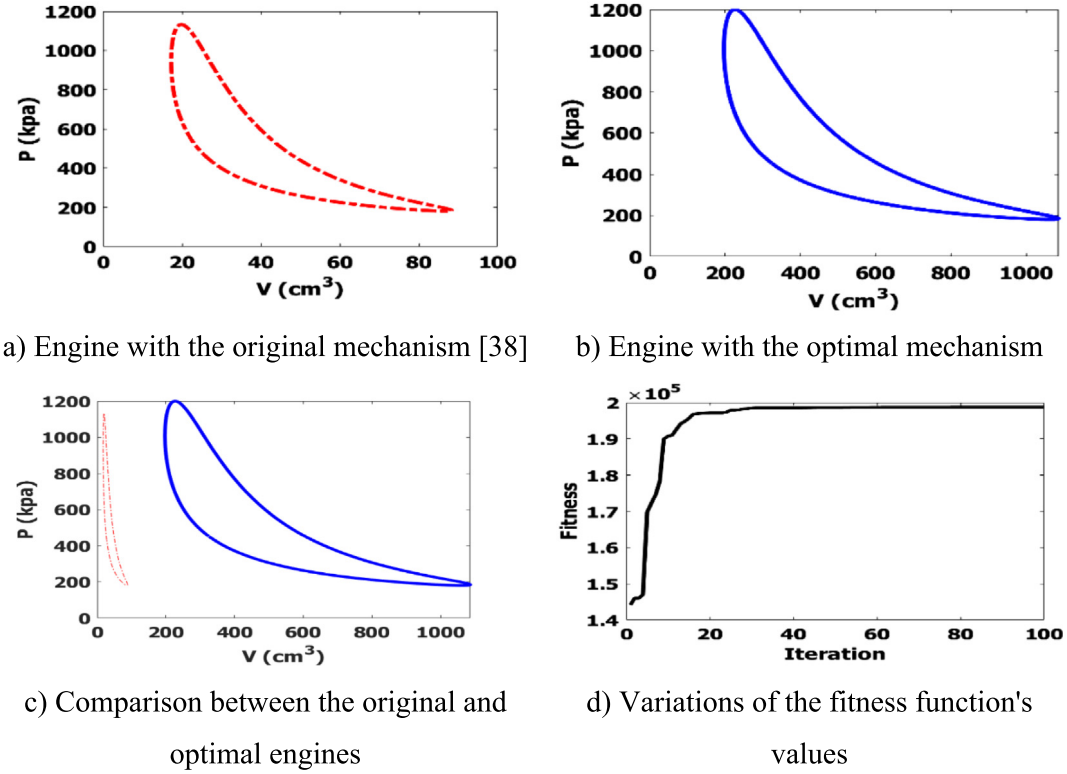

a) Engine with the original mechanism [38] b) Engine with the optimal mechanism

c) Comparison between the original and optimal engines d) Variations of the fitness function's values

Fig. 10. Optimization results of the α layout with slider-crank linkage using ICA.

The values optimum data in Table 8 for the α layout with Ross-Yoke linkage of the Stirling engine indicate that:

- Crank length (r_1) and expansion piston radius E_r reach the highest value.

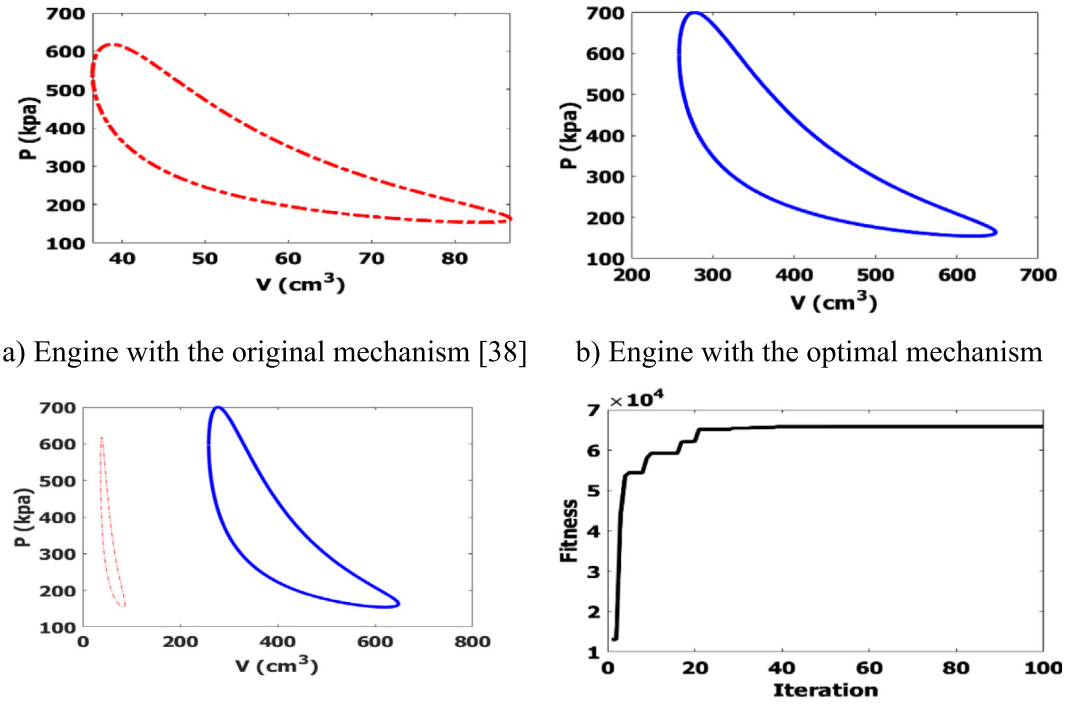

a) Engine with the original mechanism [38]

b) Engine with the optimal mechanism

c) Comparison between the original and optimal engines

d) Variations of the fitness function's values

Fig. 11. Optimization results of the β layout with slider-crank linkage using GA.

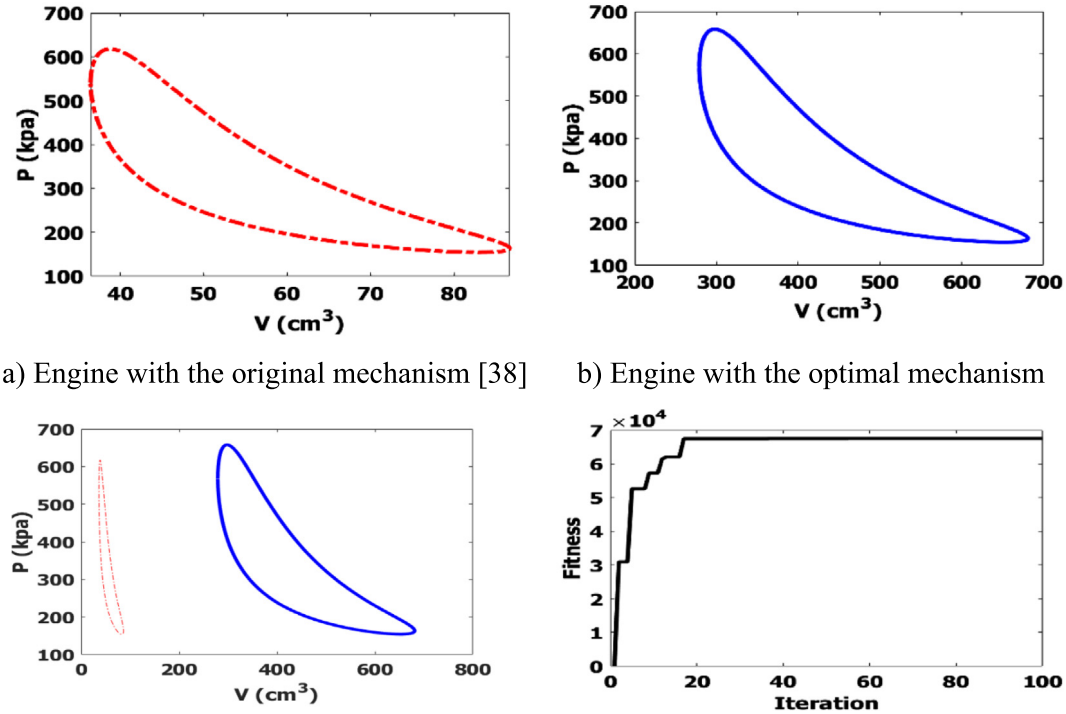

a) Engine with the original mechanism [38]

b) Engine with the optimal mechanism

c) Comparison between the original and optimal engines

d) Variations of the fitness function's values

Fig. 12. Optimization results of the β layout with slider-crank linkage using PSO.

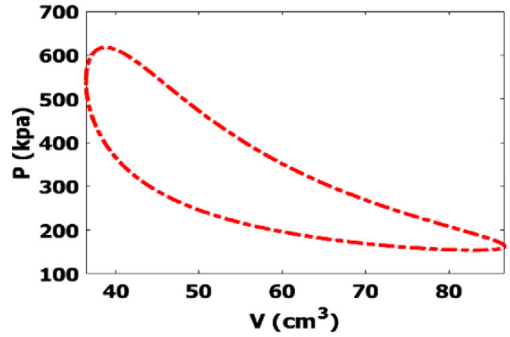

a) Engine with the original mechanism [38]

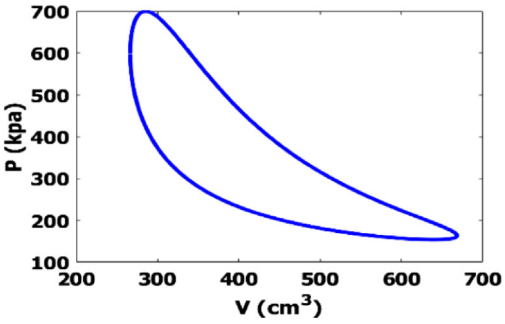

b) Engine with the optimal mechanism

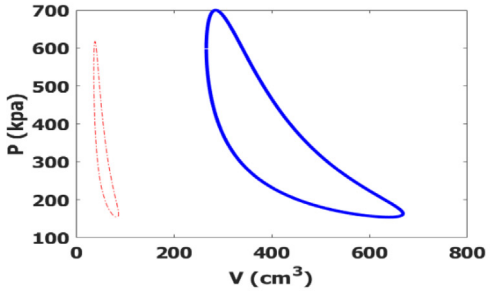

c) Comparison between the original and optimal engines

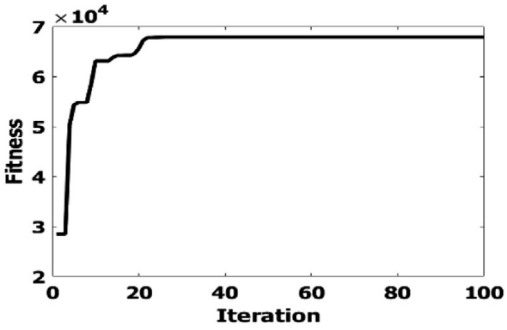

d) Variations of the fitness function's values

Fig. 13. Optimization results of the β layout with slider-crank linkage using ICA.

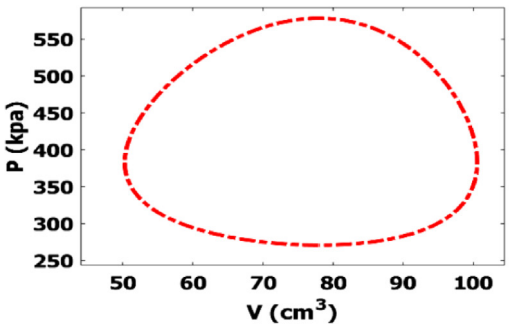

a) Engine with the original mechanism [38]

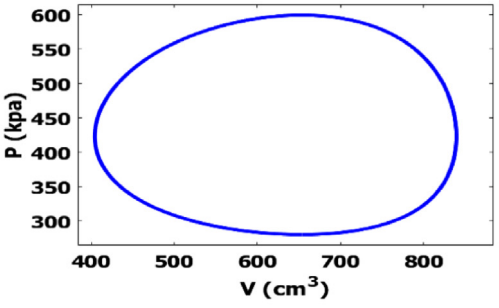

b) Engine with the optimal mechanism

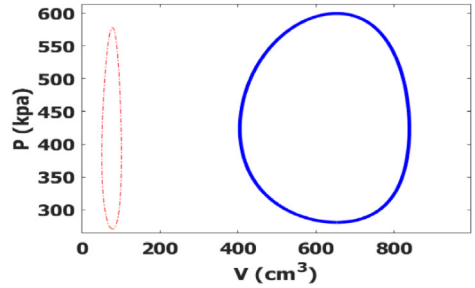

c) Comparison between the original and optimal engines

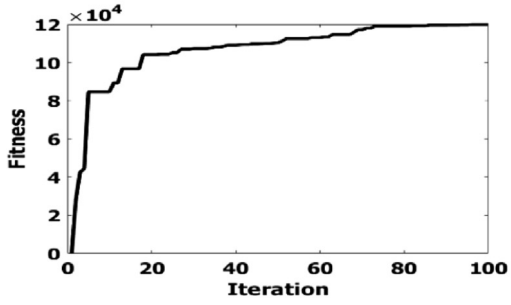

d) Variations of the fitness function's values

Fig. 14. Optimization results of the γ layout with slider-crank linkage using GA.

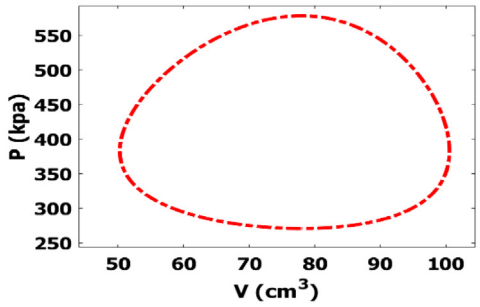

a) Engine with the original mechanism [38]

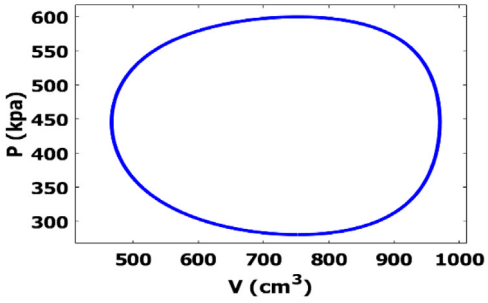

b) Engine with the optimal mechanism

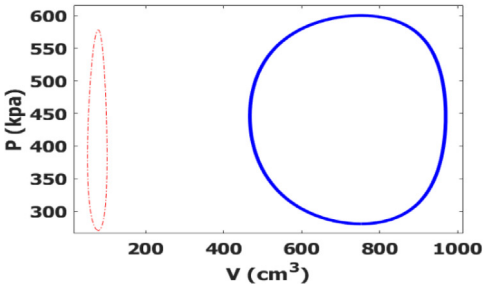

c) Comparison between the original and optimal engines

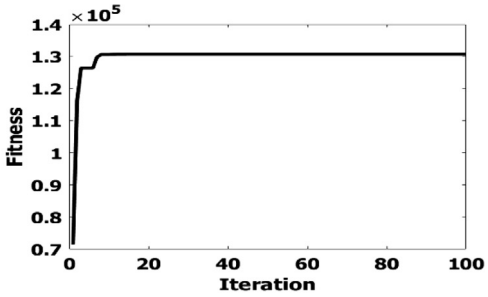

d) Variations of the fitness function's values

Fig. 15. Optimization results of the γ layout with slider-crank linkage using PSO.

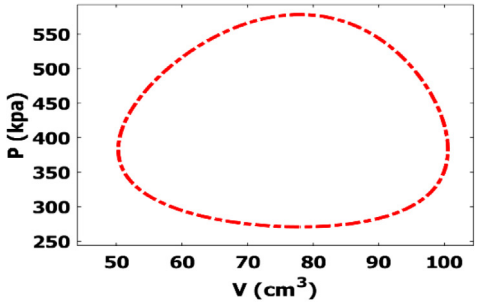

a) Engine with the original mechanism [38]

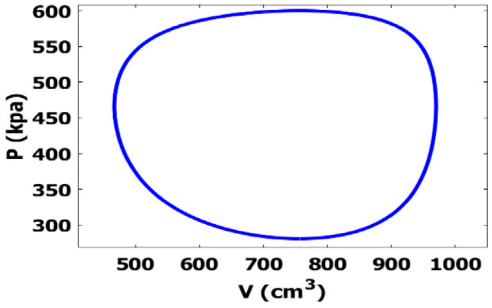

b) Engine with the optimal mechanism

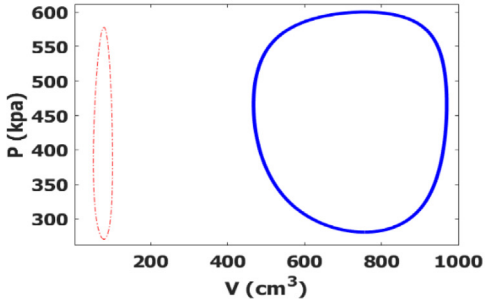

c) Comparison between the original and optimal engines

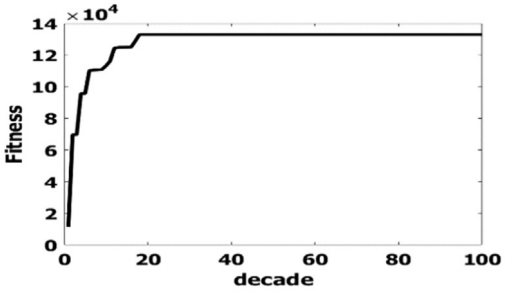

d) Variations of the fitness function's values

Fig. 16. Optimization results of the γ layout with slider-crank linkage using ICA.

Table 6
Optimal values for the variables of β type with slider-crank.

	Original values Egas and Clucas (2018)	Optimal values using GA	Optimal values using PSO	Optimal values using ICA
l_1 (cm)	13.5	27.4205	27.7482	22.6894
l_2 (cm)	10	24.5684	21.3918	25.6851
c_1 (cm)	2.1	6.08209	1.3564	4.06067
c_2 (cm)	8.5	14.0761	13.0591	6.36323
$r_1 = r_2$ (cm)	2	3.87036	4	4
E_r (cm)	2	4	4	4
W (kg (cm/s)^2)	$W_0 = 7335.8998$	65783.5783	67576.015	67896.6493
W/W$_0$	1	8.9673	9.2117	9.2554

Table 7
Optimal values for the variables of γ type with slider-crank.

	Original values Egas and Clucas (2018)	Optimal values using GA	Optimal values using PSO	Optimal values using ICA
l_1 (cm)	10	17.4575	18.8686	17.1783
l_2 (cm)	10	5.00156	7.3881	6.2952
c_2 (cm)	6.5	11.6475	11.3428	4.48347
$r_1 = r_2$ (cm)	2	5	5	5
E_r (cm)	2	3.72078	4	4
D_r (cm)	2	3.58853	3.85611	3.85611
W (kg (cm/s)^2)	$W_0 = 11935.0956$	119871.0473	130718.8482	132960.2591
W/W_0	1	10.0436	10.9525	11.1403

Table 8
Optimal values for the variables of α type with Ross-Yoke.

	Original values Egas and Clucas (2018)	Optimal values using GA	Optimal values using PSO	Optimal values using ICA
l_1 (cm)	10	11.197	8.94124	11.5195
l_2 (cm)	10	17.9108	13.8261	17.4637
r_1 (cm)	2	4	4	4
E_r (cm)	2	4	4	4
C_r (cm)	2	6.78741	6.7606	6.90844
W (kg (cm/s)^2)	W0 = 22218.6015	316245.6349	320805.9008	320335.1332
W/W_0	1	14.2334	14.4386	14.4174

- It can be found that regardless of other parameters, increasing the value of r_1 can be lead the higher output work.
- Similar to previous cases, if both E_r and C_r have increased together, it can result in higher output work; but increasing in one of these radiuses has not any improvement.
- A comparison of the results of three optimization algorithms shows that the PSO has the highest value for output work and the lowest value for l_1, and l_2. It makes it clear that the higher value for the lengths of the links not necessarily leads to higher output work.
- The output works of the optimized mechanisms extracted using three optimization techniques are approximately 14 times greater than the original mechanism.
- PSO has the best result between three optimization techniques for this layout of the Stirling engine.

The comparison between three optimization techniques (Fig. 20) for four design cases shows that PSO and ICA have better results than GA. Moreover, average improvement (between three optimization algorithms) for output work is about 13.05, 9.14, 10.71 and 14.36 times for α type with slider-crank, β type with slider-crank, γ type with slider-crank and α type with Ross-Yoke, respectively. Therefore, α layout has the best result than β and γ layouts, for maximizing the output work based on changing the geometrical parameters.

7. Conclusion

In the current study, the dimensional synthesis of the Stirling engine by considering four different layouts (α-type with slider-crank; β-type with slider-crank; γ-type with slider-crank; α-type with rose-yoke) is obtained. The engine's design and its optimization are based on the changes in the kinematics of the system. Thus, the design variables are geometrical parameters such as links length, piston radiuses, etc., and the thermodynamic parameters are fixed. The objective function is considered as the maximization of the engine's output work.

The maximum and minimum values of engine pressure for different layouts and the permissible intervals for design variables are considered as the constraints for this optimization problem. This optimization problem is solved for different layouts and using three evolutionary optimization techniques (GA, PSO, ICA). From the presented results, it can be concluded that

- The low or high-temperature difference of the Stirling engine is an intrinsic property of any layout, and even changing the length of the links, it retains this property.
- It can be found that regardless of other parameters, increasing the value of the crank length can be lead the higher output work.

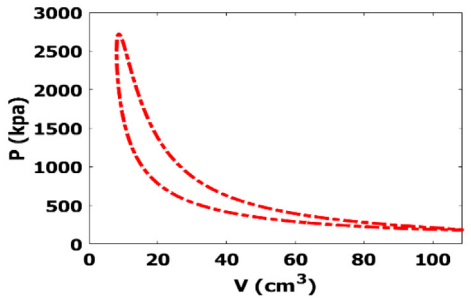

a) Engine with the original mechanism [38]

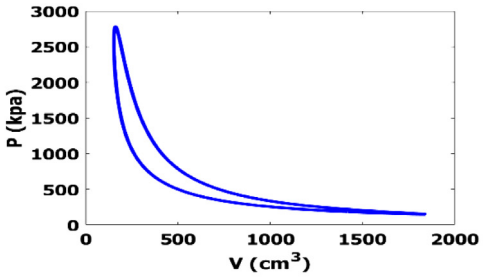

b) Engine with the optimal mechanism

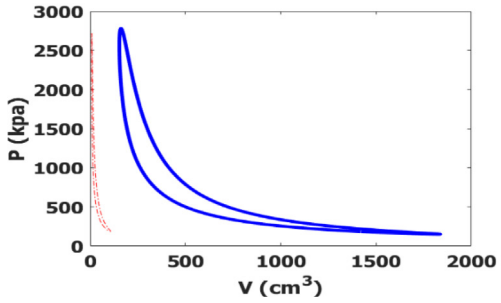

c) Comparison between the original and optimal engines

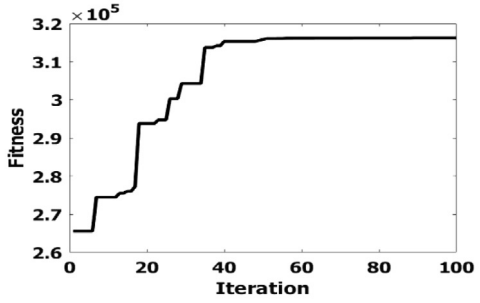

d) Variations of the fitness function's values

Fig. 17. Optimization results of the α layout with Ross-Yoke linkage using GA.

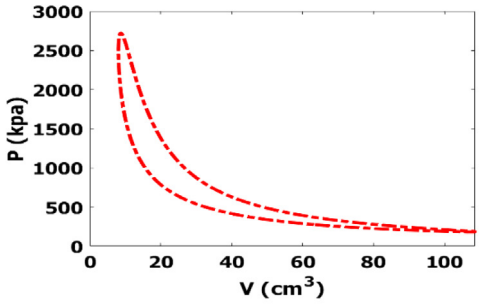

a) Engine with the original mechanism [38]

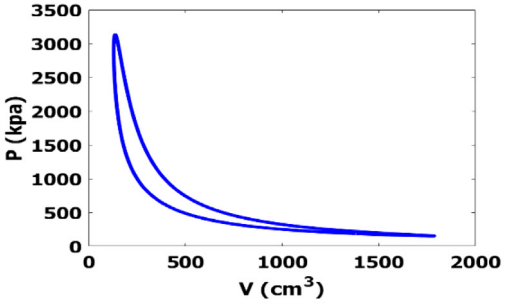

b) Engine with the optimal mechanism

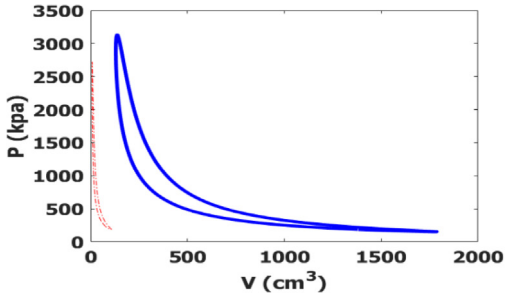

c) Comparison between the original and optimal engines

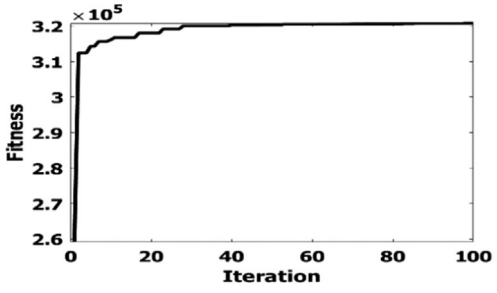

d) Variations of the fitness function's values

Fig. 18. Optimization results of the α layout with Ross-Yoke linkage using PSO.

- About the radius of the pistons, if the expansion and compression pistons radiuses are increased together, the engine's output work is improved. But, increasing in one of the two radiuses has not any good improvement.
- Results make it clear that the higher value for the lengths of the links not necessarily leads to higher output work.

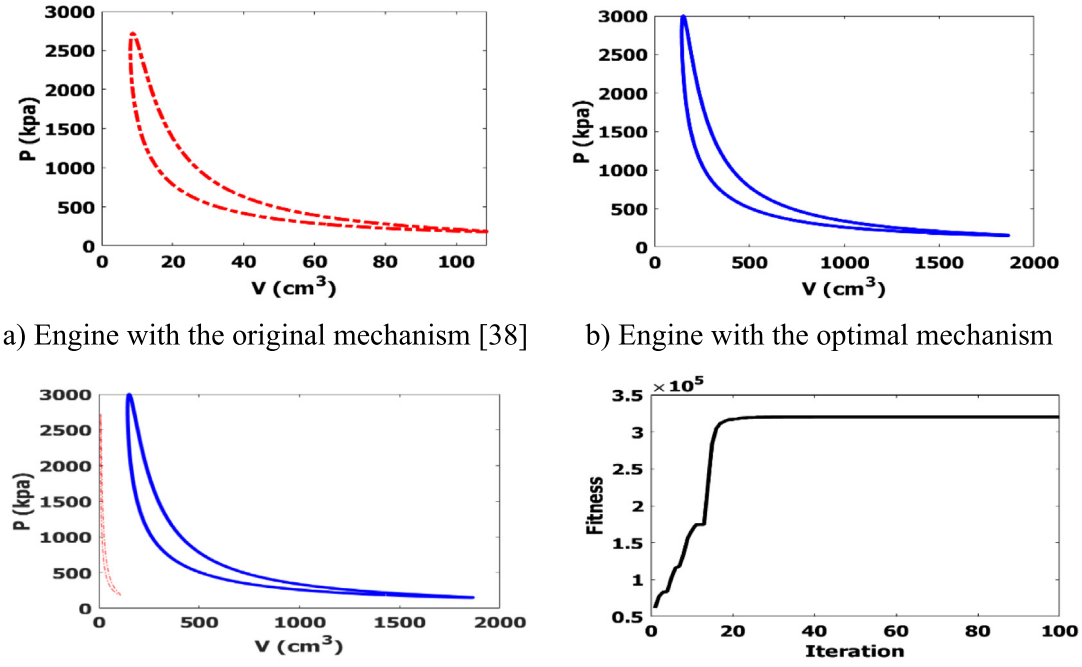

Fig. 19. Optimization results of the α layout with Ross-Yoke linkage using ICA.

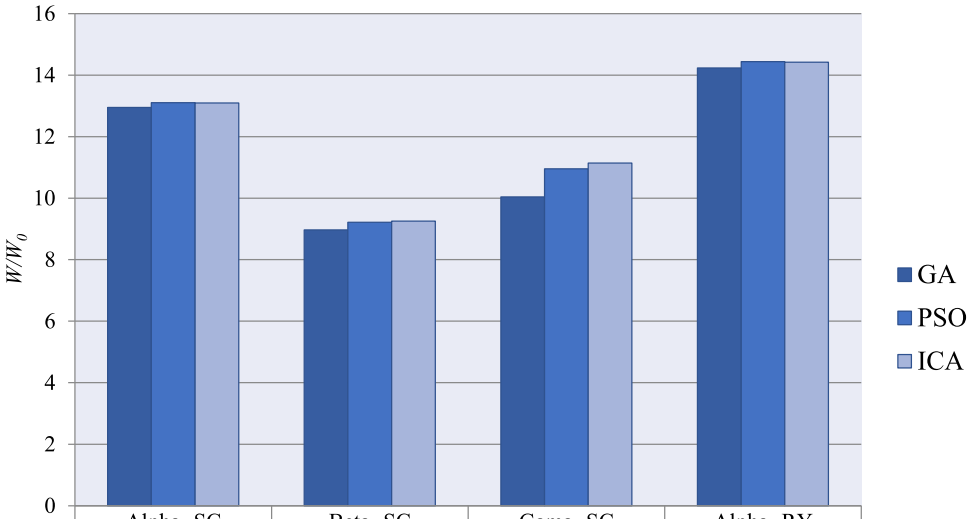

	Alpha- SC	Beta- SC	Gama- SC	Alpha- RY
GA	12.9529	8.9673	10.0436	14.2334
PSO	13.1032	9.2117	10.9525	14.4386
ICA	13.0942	9.2554	11.1403	14.4174

Fig. 20. The comparison between three optimization techniques.

- The comparison between the three optimization techniques shows that PSO and ICA have better results than GA.
- Moreover, α layout has the best result than β and γ layouts, for maximizing the output work based on changing the geometrical parameters.

CRediT authorship contribution statement

A. Rahmati: Writing - original draft, Formal analysis, Data curation, Software, Validation. **S.M. Varedi-Koulaei:** Conceptualization, Methodology, Project administration, Supervision, Validation. **M.H. Ahmadi:** Conceptualization, Supervision, Writing - review & editing. **H. Ahmadi:** Supervision, Writing - review & editing.

Declaration of competing interest

The authors declare that they have no known competing financial interests or personal relationships that could have appeared to influence the work reported in this paper.

Nomenclature

α	Phase angle
β	Crank angle
C_1	Slider length
C_2	Slider length
C_r	The radius of the compression piston
D_r	Displacement piston
E_r	The radius of the expansion piston
h	Heater
l_1	Length of the connecting rod
l_2	Length of the connecting rod
mol	The molar mass of the gas
P	Absolute pressure
P_{mean}	Engine absolute pressure in static conditions
R	The global constant of gases
r	Crank radius
T	Absolute temperature
T_c	Compression temperature
T_e	Expansion temperature
T_{room}	Room temperature
V	Volume
V_c	The volume of the compression cylinder
V_e	The volume of the expansion cylinder
V_{max}	Maximum engine volume
W	Output work
W_0	Output work of the original mechanism
x	Vector of design variables
x_{max}	The upper bound of the design variables
x_{min}	The lower bound of the design variables

Acknowledgment

This research did not receive any specific grant from funding agencies in the public, commercial, or not-for-profit sectors.

References

Abuelyamen, A., Ben-Mansour, R., Abualhamayel, H., Mokheimer, E.M.A., 2017. Parametric study on beta-type Stirling engine. Energy Convers. Manage. 145, 53–63. http://dx.doi.org/10.1016/J.ENCONMAN.2017.04.098.

Ahmadi, M.H., Ahmadi, M.A., Mellit, A., Pourfayaz, F., Feidt, M., 2016. Thermodynamic analysis and multi objective optimization of performance of solar dish Stirling engine by the centrality of entransy and entropy generation. Int. J. Electr. Power Energy Syst. 78, 88–95. http://dx.doi.org/10.1016/J.IJEPES.2015.11.042.

Ahmadi, M.H., Ahmadi, M.-A., Pourfayaz, F., 2017. Thermal models for analysis of performance of stirling engine: A review. Renew. Sustain. Energy Rev. 68, 168–184. http://dx.doi.org/10.1016/J.RSER.2016.09.033.

Ahmadi, M.H., Alhuyi Nazari, M., Sadeghzadeh, M., Pourfayaz, F., Ghazvini, M., Ming, T., et al., 2019. Thermodynamic and economic analysis of performance evaluation of all the thermal power plants: A review. Energy Sci. Eng. 7, 30–65. http://dx.doi.org/10.1002/ese3.223.

Ahmadi, M.H., Ghazvini, M., Sadeghzadeh, M., Alhuyi Nazari, M., Kumar, R., Naeimi, A., et al., 2018. Solar power technology for electricity generation: A critical review. Energy Sci. Eng. 1–22. http://dx.doi.org/10.1002/ese3.239.

Ahmadi, M.H., Hosseinzade, H., Sayyaadi, H., Mohammadi, A.H., Kimiaghalam, F., 2013b. Application of the multi-objective optimization method for designing a powered Stirling heat engine: Design with maximized power, thermal efficiency and minimized pressure loss. Renew. Energy 60, 313–322. http://dx.doi.org/10.1016/J.RENENE.2013.05.005.

Ahmadi, M.H., Mohammadi, A.H., Dehghani, S., Barranco-Jiménez, M.A., 2013d. Multi-objective thermodynamic-based optimization of output power of Solar Dish-Stirling engine by implementing an evolutionary algorithm. Energy Convers. Manage. 75, 438–445. http://dx.doi.org/10.1016/J.ENCONMAN.2013.06.030.

Ahmadi, M.H., Sayyaadi, H., Dehghani, S., Hosseinzade, H., 2013a. Designing a solar powered Stirling heat engine based on multiple criteria: Maximized thermal efficiency and power. Energy Convers. Manage. 75, 282–291. http://dx.doi.org/10.1016/J.ENCONMAN.2013.06.025.

Ahmadi, M.H., Sayyaadi, H., Mohammadi, A.H., Barranco-Jimenez, M.A., 2013c. Thermo-economic multi-objective optimization of solar dish-Stirling engine by implementing evolutionary algorithm. Energy Convers. Manage. 73, 370–380. http://dx.doi.org/10.1016/J.ENCONMAN.2013.05.031.

Almajri, A.K., Mahmoud, S., Al-Dadah, R., 2017. Modelling and parametric study of an efficient Alpha type Stirling engine performance based on 3D CFD analysis. Energy Convers. Manage. 145, 93–106. http://dx.doi.org/10.1016/J.ENCONMAN.2017.04.073.

Altin, M., Okur, M., Ipci, D., Halis, S., Karabulut, H., 2018. Thermodynamic and dynamic analysis of an alpha type Stirling engine with Scotch Yoke mechanism. Energy 148, 855–865. http://dx.doi.org/10.1016/J.ENERGY.2018.01.183.

Atashpaz-Gargari, E., Lucas, C., 2007. Imperialist competitive algorithm: an algorithm for optimization inspired by imperialistic competition. In: 2007 IEEE Congress on Evolutionary Computation. pp. 4661–4667. http://dx.doi.org/10.1109/CEC.2007.4425083.

Babaelahi, M., Sayyaadi, H., 2014. Simple-II: A new numerical thermal model for predicting thermal performance of Stirling engines. Energy 69, 873–890. http://dx.doi.org/10.1016/J.ENERGY.2014.03.084.

Bataineh, K., 2018. Mathematical formulation of alpha -type Stirling engine with Ross Yoke mechanism. Energy 164, 1178–1199. http://dx.doi.org/10.1016/J.ENERGY.2018.08.134.

Bayón, L., Grau, J.M., Suarez, P., 2002. A new formulation of the equivalent thermal in optimization of hydrothermal systems. Math. Probl. Eng. 8, 181–196.

Bayon, L.F., Suarez, P.M., 2000. Multiple objective optimization of hydro-thermal systems using Rit'z method. Math. Probl. Eng. 5, 379–396.

Boubaker, K., Colantoni, A., Longo, L., Menghini, G., Baciotti, B., Allegrini, E., et al., 2013. Optimizing the energy conversion process: An application to a biomass gasifier-stirling engine coupling system. Appl. Math. Sci. 7, 6931–6944. http://dx.doi.org/10.12988/ams.2013.310567.

Cheng, C.-H., Yu, Y.-J., 2011. Dynamic simulation of a beta-type Stirling engine with cam-drive mechanism via the combination of the thermodynamic and dynamic models. Renew. Energy 36, 714–725. http://dx.doi.org/10.1016/J.RENENE.2010.07.023.

Cheng, C.-H., Yu, Y.-J., 2012. Combining dynamic and thermodynamic models for dynamic simulation of a beta-type Stirling engine with rhombic-drive mechanism. Renew. Energy 37, 161–173. http://dx.doi.org/10.1016/J.RENENE.2011.06.013.

Deac, I.G., 1994. Deac IG design and performance test of a miniature stirling cryocooler. Cryogenics (Guildf) 34, 191–193. http://dx.doi.org/10.1016/S0011-2275(05)80040-2.

Ding, G., Chen, W., Zheng, T., Li, Y., Ji, Y., 2018. Volume ratio optimization of stirling engine by using an enhanced model. Appl. Therm. Eng. 140, 615–621. http://dx.doi.org/10.1016/j.applthermaleng.2018.04.067.

Duan, C., Wang, X., Shu, S., Jing, C., Chang, H., 2014. Thermodynamic design of stirling engine using multi-objective particle swarm optimization algorithm. Energy Convers. Manage. 84, 88–96. http://dx.doi.org/10.1016/J.ENCONMAN.2014.04.003.

Egas, J., Clucas, D.M., 2018. Stirling engine configuration selection. Energies 11 (3), 584. http://dx.doi.org/10.3390/en11030584.

Finkelstein, T., 0000. Insights into the thermodynamics of Stirling cycle machines. In: Intersoc. Energy Convers. Eng. Conf. n.d. http://dx.doi.org/10.2514/6.1994-3951.

Hachem, H., Gheith, R., Aloui, F., Ben Nasrallah, S., 2018. Technological challenges and optimization efforts of the Stirling machine: A review. Energy Convers. Manage. 171, 1365–1387. http://dx.doi.org/10.1016/J.ENCONMAN.2018.06.042.

Holl, J.H., 1975. Adaptation in Natural and Artificial Systems, Vol. 100. University of Michigan Press, ann arbor.

Hooshang, M., Moghadam, R.Askari., Alizadeh Nia, S., Masouleh, M.T., 2015. Optimization of Stirling engine design parameters using neural networks. Renew. Energy 74, 855–866. http://dx.doi.org/10.1016/J.RENENE.2014.09.012.

Karabulut, H., Okur, M., Ozdemir, A.O., 2019. Performance prediction of a martini type of stirling engine. Energy Convers. Manage. 179, 1–12. http://dx.doi.org/10.1016/j.enconman.2018.10.059.

Kennedy, J., R., Eberhart, 1995. Particle swarm optimization. In: Proceedings of ICNN'95-International Conference on Neural Networks, Vol. 4. pp. 1942–1948. http://dx.doi.org/10.1109/ICNN.1995.488968.

Kongtragool, B., Wongwises, S., 2003. A review of solar-powered stirling engines and low temperature differential Stirling engines. Renew. Sustain. Energy Rev. 7, 131–154. http://dx.doi.org/10.1016/S1364-0321(02)00053-9.

Kraitong, K., Mahkamov, K., 2011. Optimisation of low temperature difference solar stirling engines using genetic algorithm. In: World Renewable Energy Congress-Sweden, Vol. 057. 8–13 May; 2011; Linköping; Sweden, pp. 3945–3952. http://dx.doi.org/10.3384/ecp110573945.

Liao, T., Lin, J., 2015. Optimum performance characteristics of a solar-driven Stirling heat engine system. Energy Convers. Manage. 97, 20–25. http://dx.doi.org/10.1016/J.ENCONMAN.2015.03.027.

Martini, W., 1983. Stirling engine design manual conservation and renewable energy. methods. 412.

Motsa, S., Shateyi, S., 2012. Successive linearization analysis of the effects of partial slip, thermal diffusion, and diffusion-thermo on steady MHD convective flow due to a rotating disk. Math. Probl. Eng. 15, http://dx.doi.org/10.1155/2012/397637.

Praveen, C., Duvigneau, R., 2009. Low cost PSO using metamodels and inexact pre-evaluation: Application to aerodynamic shape design. Comput. Methods Appl. Mech. Eng. 198 (9–12), 1087–1096. http://dx.doi.org/10.1016/j.cma.2008.11.019.

Rao, S.S., 2019. Engineering Optimization: Theory and Practice, fourth ed. John Wiley & Sons.

Rao, R.V., Keesari, H.S., Oclon, P., Taler, J., 2019. Improved multi-objective Jaya optimization algorithm for a solar dish Stirling engine. J. Renew. Sustain. Energy 11 (2), 025903. http://dx.doi.org/10.1016/j.ijepes.2015.11.042.

S, L., Alí´a de, S.D., Echazú´, R., y Alcorta, G., 2007. La Simulacion de Sistemas Termomecánicos Solares Con El Programa Simusol, Vol. 11. El Motor Stirling : Simulacion Y Construcción, pp. 1–8.

S. Scollo, L., E. Valdez, P., R. Santamarina, S., R. Chini, M., H. Baron, J., 2013. Twin cylinder alpha stirling engine combined model and prototype redesign. Int. J. Hydrogen Energy 38, 1988–1996. http://dx.doi.org/10.1016/j.ijhydene.2012.01.180.

Sardashti, A., Daniali, H.M., Varedi, S.M., 2013. Optimal free-defect synthesis of four-bar linkage with joint clearance using PSO algorithm. Meccanica 48 (7), 1681–1693. http://dx.doi.org/10.1007/s11012-013-9699-6.

Schmidt, G., 1871. The theory of lehmann's Calorimetric machine. 15. ZVereinesDeutcherIngenieure.

Shendage, D., Kedare, S., Bapat, S., 2017. Cyclic analysis and optimization of design parameters for beta-configuration stirling engine using rhombic drive. Appl. Therm. Eng. 124, 595–615. http://dx.doi.org/10.1016/j.applthermaleng.2017.06.075.

Thombare, D.G., Verma, S.K., 2008. Technological development in the Stirling cycle engines. Renew. Sustain. Energy Rev. 12, 1–38. http://dx.doi.org/10.1016/J.RSER.2006.07.001.

Tlili, I., Timoumi, Y., Ben, Nasrallah S., 2008. Analysis and design consideration of mean temperature differential Stirling engine for solar application. Renew. Energy 33, 1911–1921. http://dx.doi.org/10.1016/J.RENENE.2007.09.024.

Toghyani, S., Kasaeian, A., Hashemabadi, S.H., Salimi, M., 2014. Multi-objective optimization of GPU3 stirling engine using third order analysis. Energy Convers. Manage. 87, 521–529. http://dx.doi.org/10.1016/J.ENCONMAN.2014.06.066.

Urieli, I., Berchowitz, D., 1984. Stirling Cycle Engine Analysis. Adam Hilger, Bristol.

Walker, G., 1980. Stirling Engines. Claredon Press, Oxford.

Wang, K., Sanders, S.R., Dubey, S., Choo, F.H., Duan, F., 2016. Stirling cycle engines for recovering low and moderate temperature heat: A review. Renew. Sustain. Energy Rev. 62, 89–108. http://dx.doi.org/10.1016/J.RSER.2016.04.031.

Woon, S.Y., Tong, L., Querin, O.M., Steven, G.P., 2005. Effective optimisation of continuum topologies through a multi-GA system. Comput. Methods Appl. Mech. Engrg. 194 (30–33), 3416–3437. http://dx.doi.org/10.1016/j.cma.2004.12.025.

Xiao, G., Sultan, U., Ni, M., Peng, H., Zhou, X., Wang, S., Luo, Z., 2017b. Design optimization with computational fluid dynamic analysis of β-type Stirling engine. Appl. Therm. Eng. 113, 87–102. http://dx.doi.org/10.1016/j.applthermaleng.2016.10.063.

Xiao, G., Sultan, U., Ni, M., Peng, H., Zhou, X., Wang, S., et al., 2017a. Design optimization with computational fluid dynamic analysis of β-type Stirling engine. Appl. Therm. Eng. 113, 87–102. http://dx.doi.org/10.1016/J.APPLTHERMALENG.2016.10.063.